

Novel Fork Architectures of Ag₂S Nanoparticles Synthesized Through In-Situ Self-Assembly Inside Chitosan Matrix

Lubna Hashmi^{1a*}, Prabha Sana^{1b}, M. M. Malik^{1c}, A. H. Siddiqui^{2d}
and M.S.Qureshi^{1e}

¹Dept of Physics, Maulana Azad National Institute of Technology, Bhopal (M.P.), 462051, INDIA

²Dept. of Physics, Jawahar Lal Nehru P.G. College, Shyamla Hills, Bhopal (M.P.), INDIA

e-mail: ^alubna_hash@yahoo.co.in(Corresponding Author), ^bprabhasana@yahoo.co.in ,

^cmanzar.mailk@gmail.com , ^daamirhusainsiddiqui@yahoo.co.in,

^eshumsqureshi@rediffmail.com

Keywords: Ag₂S nanoparticles, Chitosan, Self-assembly, Ag₂S-Chitosan, Fork Structure.

Abstract. In a simple reaction between Silver nitrate and Thiourea under the presence of Chitosan, novel fork architectures of silver sulfide (Ag₂S) were obtained through *In-situ* self- assembly of Ag₂S nanoparticles inside Chitosan matrix in aqueous basic environment. Samples were characterized by SEM, TEM, XRD, FTIR, Raman Spectroscopy and UV-vis Spectroscopy. Average particle size was found to be 8 nm from TEM analysis. Formation of crystalline monoclinic α -Ag₂S was confirmed by SAED and X-ray diffraction analysis. The experimental results show that the fork architectures of Ag₂S can be obtained from Tape like assemblies of Ag₂S nanoparticles at the later stage of their growth with temperature. Raman spectra confirm the incorporation of Ag₂S nanoparticles inside Chitosan matrix. Multiple resonant Raman peaks indicates that the yielded Ag₂S nanoparticles possess good optical quality and crystallinity. FTIR spectra indicates that the Ag⁺ ion is coupled with the C=O bond of the Chitosan molecules through the electrostatic interaction. UV-vis absorption spectrum of the Ag₂S Fork architectures has a broad absorption band in the UV to visible region, and the blue-shifting of the band is observed along with the presence of both direct and indirect band gap.

Introduction

Assembly and hierarchical structuring of nanomaterials is a technologically driven area of research due to the opportunities it provides for applications ranging from material science through to molecular biology [1]. Self-assembly seems to offer one of the most general strategies now available for generating nanostructures [2]. A range of recent research efforts have focused on various self-assembly strategies to control the organization of nanoparticles building blocks in colloidal media [3-15]. Silver sulfide (Ag_2S NPs), a semiconductor has recently received considerable attention due to its potentially wide applications in nanoscale systems. Ag_2S is an important semiconductor with good chemical stability and optical limiting properties that has potential applications as a photoelectric and thermoelectric material [16], IR detectors and super ionic conductors [17-19]. These unique properties suggest its potentially broad applications as nanoparticles and its nanocomposites. For many of these applications, the assembly of semiconductor nanoparticles into well-defined superstructures is critically important. Furthermore, the assemblies may produce new properties that differ from those of single nanoparticle, arising from the spatial orientation and network arrangement [20-22].

Self-assembly of Ag_2S NPs from liquid suspensions have been achieved by evaporation of solvents from the suspensions at high temperature. This technique was found to be strongly dependent on the conditions of sample preparation [20], being influenced by the length of thiol alkyl chain of coating agents [21], reaction temperature, and the thiol concentration [23]. Ag_2S NPs assemblies were also produced by exposing prefabricated monolayer of Ag nanoparticles to pure H_2S but these assemblies do not possess any perfect architecture [24]. It was also found that Ag_2S NPs when synthesized in a polymer matrix were usually of irregular shape and had a large size distribution [25, 26] therefore self assembly do not result in nano architecture formation. Therefore to obtain assemblies of Ag_2S NPs, there is a need to develop an alternate route and search for a better matrix. Hence present work was carried out to put some efforts in this field by extending the research

which involves *in situ* nucleation of Silver sulfide nanoparticles inside a polymer matrix. Since Cationic surfactants were found effective stabilizers for Ag_2S [27] and Ag_2S nanoparticles capped by NH_2 group were found to result in self assembly [28], a polymer matrix with these properties was needed. Owing to the abundance of free amine groups on Chitosan, its reactivity [29] and solubility as a function of pH and good chelating ability with transition metal ions [30] along with its non toxic nature, make this polymer to be used as a polymer matrix in the present work. Chitosan is the deacetylated product of chitin, which is an abundantly present macromolecule in crustacean exoskeleton (shrimp, crab, etc.). The monomer unit in chitosan is glucosamine (2-amino-2-deoxy-D-gluco-pyranose).

This paper describes a simple method to obtain the assemblies of Ag_2S nanoparticles by *In-situ* reaction of Silver nitrate with $\text{CS}(\text{NH}_2)_2$ (Thiourea) at 60 °C in vacuum inside Chitosan matrix. Novel Fork architectures were formed from self-assembly of Ag_2S spherical nanoparticles with average diameter 8 nm. Transformational changes were observed as a function of temperature by collecting three aliquots of colloids at 60 °C, 80 °C and 100 °C temperature, which indicate formation of fork structures from tape like structures with increasing temperature. The growth and self-assembly of Ag_2S tape and fork architectures were investigated and their possible growth mechanism is discussed.

Experimental Details

0.2% Chitosan solution was prepared in 1% acetic acid. 4 mmole AgNO_3 solution and 2 mmole Thiourea (Tu) solution was prepared in certain amount of ultra pure water. The above prepared Chitosan and AgNO_3 solution was mixed, then pH of this mixed solution was adjusted to 10 using 1 % aqueous ammonia. After mixing, the solution was taken in three neck reaction vessel and this vessel was kept in dark place and stirred for 4 h under vacuum (10^{-3} torr) at room temperature. After being stirred for 4 hrs, the mixed solution was kept at 60 °C under constant stirring. When the temperature inside the reaction vessel attains 60 °C, the prepared Tu solution was injected inside.

Ag₂S precursors are formed at this stage which is accompanying by a change of solution color to light brown and first aliquot was taken just after addition of Tu. This solution was then left to reflux in an open-air condition with condenser attached, at 80 °C and 100 °C for 30 minutes and collecting aliquots respectively. The precipitates were obtained after consecutive centrifuging (500 rpm) and vortexing several times with de-ionized water to remove any diffluent salts. Finally the precipitates were vacuum dried in vacuum desiccator.

Results and Discussion

Instrumentation. Crystallinity and purity of the samples were studied by X-ray diffraction (XRD) analysis on Rigaku Mini Flex 2 Desktop diffractometer using Cu K α radiation. The fork and tape images were taken using scanning electron microscope on a JEOL/EO version -1 model JSM-6390. The Ag₂S nanoparticles were characterized by transmission electron microscopy on a TECNAI 20 G2 microscope with an acceleration voltage of 200 kV, using W/LaB6 Filament at Room Temperature. Fourier transform infrared (FTIR) spectra of the colloids were recorded using a Perkin-Elmer FTIR Spectra-BX Spectrometer. Room temperature Raman Spectra was collected using Jobin Yvon Horiba HR 100 Raman Spectroscope. Argon laser with wavelength 488 nm was used as source of excitation at 10 mW power with Hole diameter 1000 μ m and slit width 500 μ m using Grating 1800. UV/vis spectra were recorded on ECIL-GS5705 Spectrometer. Samples for UV/vis spectroscopy and Raman Spectroscopy were prepared by diluting the colloidal samples in 10% v/v with di-water.

Microscopic Characterization of Ag₂S fork Architectures. Fig. 1 presents the SEM images of aliquots collected at 60 °C (Fig. 1(a-b)), 80 °C (Fig. 1(c-f)) and 100 °C (Fig. 1(g-h)). It is clear from these images that initially at 60 °C non uniform tape like Ag₂S assemblies were formed (Fig. 1(a-b)), as temperature reaches to 80 °C these tapes get more precise with uniformity and developed flat head at one end with multiple armed structure, which resembles fork, hence fork Ag₂S architectures were formed. When the temperature were increased to 100 °C; the length of the tail portion of the forks increases significantly (Fig 1(g)).

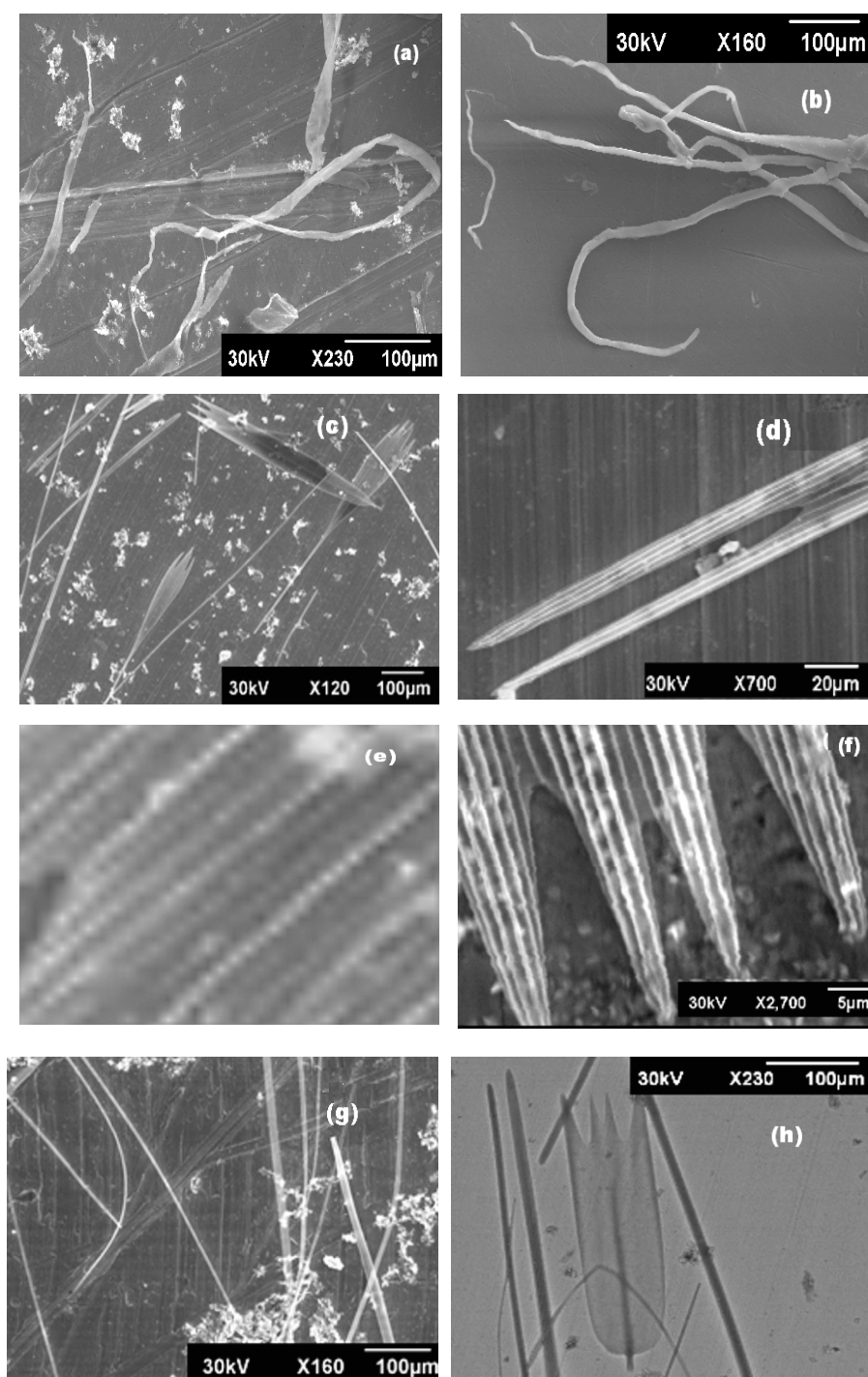


Fig. 1. SEM images of Ag_2S assemblies: (a-b) Ag_2S Tapes at 60 °C, (c-d) Ag_2S Fork architectures at 80 °C, (e-f) magnified image of Ag_2S Fork architectures achieved at 80 °C, (g-h) Ag_2S Fork architectures with longer tail at 100 °C.

Fig. 2(a) shows a typical TEM image of the product, indicating the formation of spherical Ag_2S nanoparticles, well separated from each other indicating that they are effectively stabilized by chitosan, which was further confirmed using FTIR and Raman Spectroscopy. The mean particle diameter for the Ag_2S NPs is 8 nm, calculated from 100 particles in the TEM images and its particle size distribution is given in Fig. 2(c) with standard deviation (σ) of 2.217.

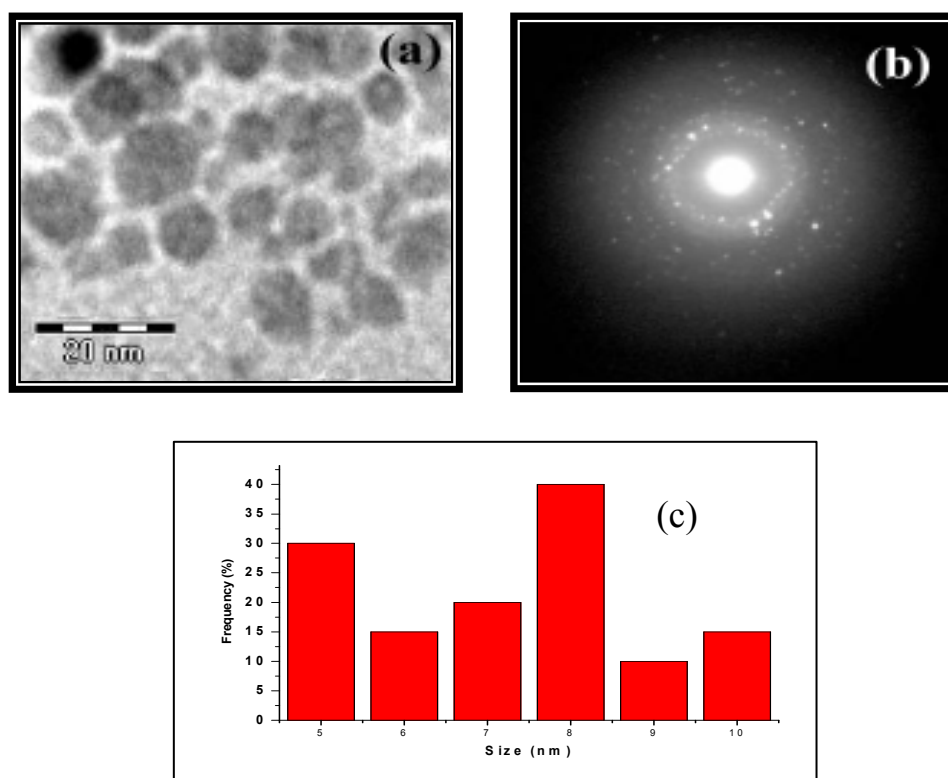


Fig. 2. (a) TEM Image of Ag_2S nanoparticles, (b) SAED Pattern of Ag_2S nanoparticles and (c) Particle size Distribution.

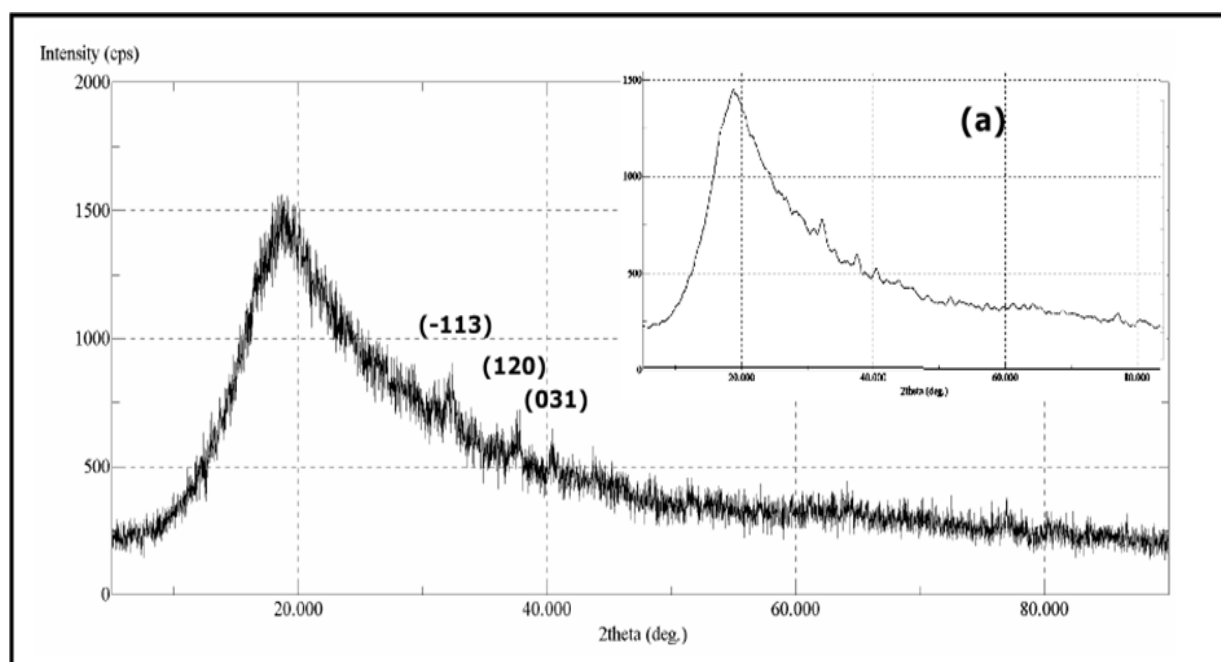


Fig. 3. XRD Pattern of Ag₂S fork Architecture

X-ray diffractogram of the precipitate extracted from colloidal suspension is shown in Fig. 1 and the peaks indexed, as referenced from JCPDS file no. 14-0072, corresponds to Monoclinic Acanthite α -Ag₂S. No impurities can be detected in this pattern. This indicates that crystalline Ag₂S is formed. The broadening of these diffraction peaks suggests that the samples are in nano size. More information about the crystallinity and the size of the particles were found in the transmission electron microscopy (TEM) study, accompanied by selected-area electron diffraction (SAED) analysis. The typical SAED pattern shown in Fig. 2 b, consist of spotted rings which indicate the co-existence of polycrystals with single crystal domains of Ag₂S as already reported earlier [24]. The d -spacings and the relative intensities of the diffraction rings of the Ag₂S NPs are found to be consistent with those reported for monoclinic acanthite [31], which is the most stable polymorph of Ag₂S at ambient temperature.

Optical characterization of Ag₂S fork Architectures. Fig. 4(a-b) shows FTIR spectra of pure Chitosan 0.2% solution and Ag₂S fork architectures respectively.

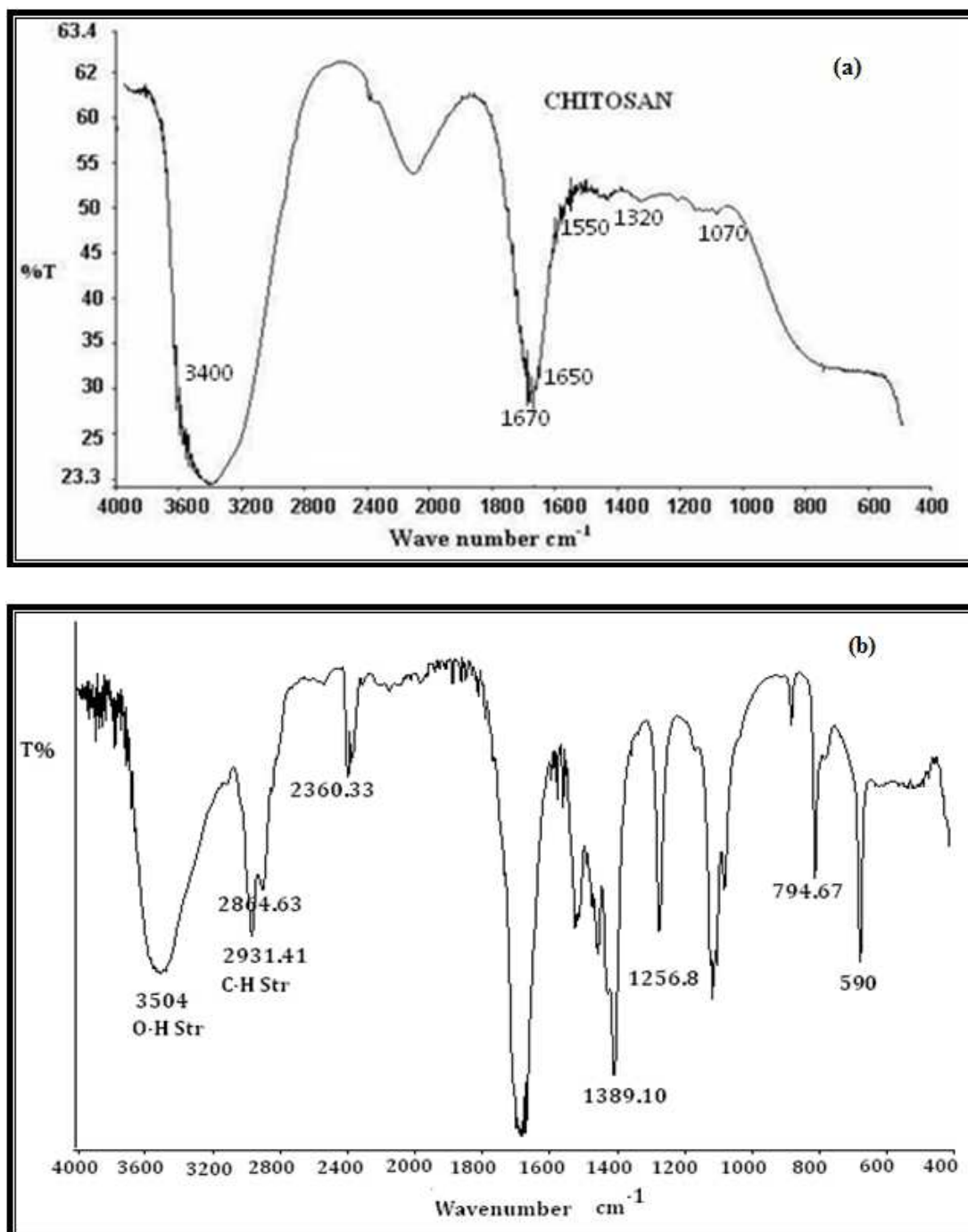


Fig. 4. FTIR spectra of (a) chitosan 0.2% solution and (b) Ag₂S fork architectures.

In Fig. 4(a), spectral deformation band at 3400 cm⁻¹ for the OH⁻ groups, convoluted peak at 2900 cm⁻¹ for the -CH₂ backbone, 1650–1690 cm⁻¹ for the amide I (C=O) bands, there is another convoluted spectral peak at around 1650 -1550 cm⁻¹, which are assigned to amine (-NH₂), convoluted

peak at 1550cm^{-1} is assigned for the amide II ($-\text{NH}$) and around 1320 cm^{-1} for the amide III. The shoulder peaks observed at 1070 and 894 cm^{-1} are attributed for the stretching vibration of $\text{C}-\text{O}-\text{C}$ linkages in the saccharide structure of chitosan. All the bands described above were also observed for the Ag_2S fork architectures as depicted in Fig. 4(b). Formation of Chitosan -silver sulfide composite shifted the O-H Stretch band from 3400 cm^{-1} to 3504 cm^{-1} with evolution of a peak at 2931 cm^{-1} and having shoulder at 2864 cm^{-1} for CH_2 backbone of chitosan. The characteristic peak of amide get shifted from 1670 cm^{-1} to 1650 cm^{-1} and ensures the incorporation of silver ions into the Chitosan matrix. A shift in $\text{C}=\text{O}$ absorption band was due to the interaction between silver ions and the carbonyl groups in Chitosan. This interaction may be attributed to the donation of a pair of electrons from the carbonyl oxygen to the silver cations, called inductive effect [32]. This result suggests that the nucleation and self-organization of Ag_2S nanocrystals can be controlled by the Chitosan macromolecules, and the carbonyl groups on the surface of the Chitosan molecules can be the nucleation sites of Ag_2S . Ag_2S nanocrystals precipitated on the surface of the Chitosan macromolecules and are spontaneously formed into tape and fork architectures.

Moreover, Raman spectroscopy can also provide valuable structural information on semiconductor nanostructures [33]. However, until now, there has been little work reported on the Raman characterization of Silver sulfide nanoparticles. Fig. 5(a) shows the room temperature Raman spectra of the yielded silver sulfide Fork assemblies. Broadening of the peaks in spectra indicate the formation of nanoparticles. Broad feature peak around 250 cm^{-1} is indicative of the Ag-S bond at the surface [34], hence confirms the formation of Ag_2S nanocrystals. It is noticed that strong resonant Raman scattering with high-order longitudinal optical (LO) modes are obtained. Strong fundamental and weak overtone modes are detected at 213.5 cm^{-1} and 427 cm^{-1} respectively [35] which correspond to the first order longitudinal optical phonon modes (1LO) and second order longitudinal optical phonon modes (2LO) in Ag_2S respectively and are the result of phonon vibration [36-38].

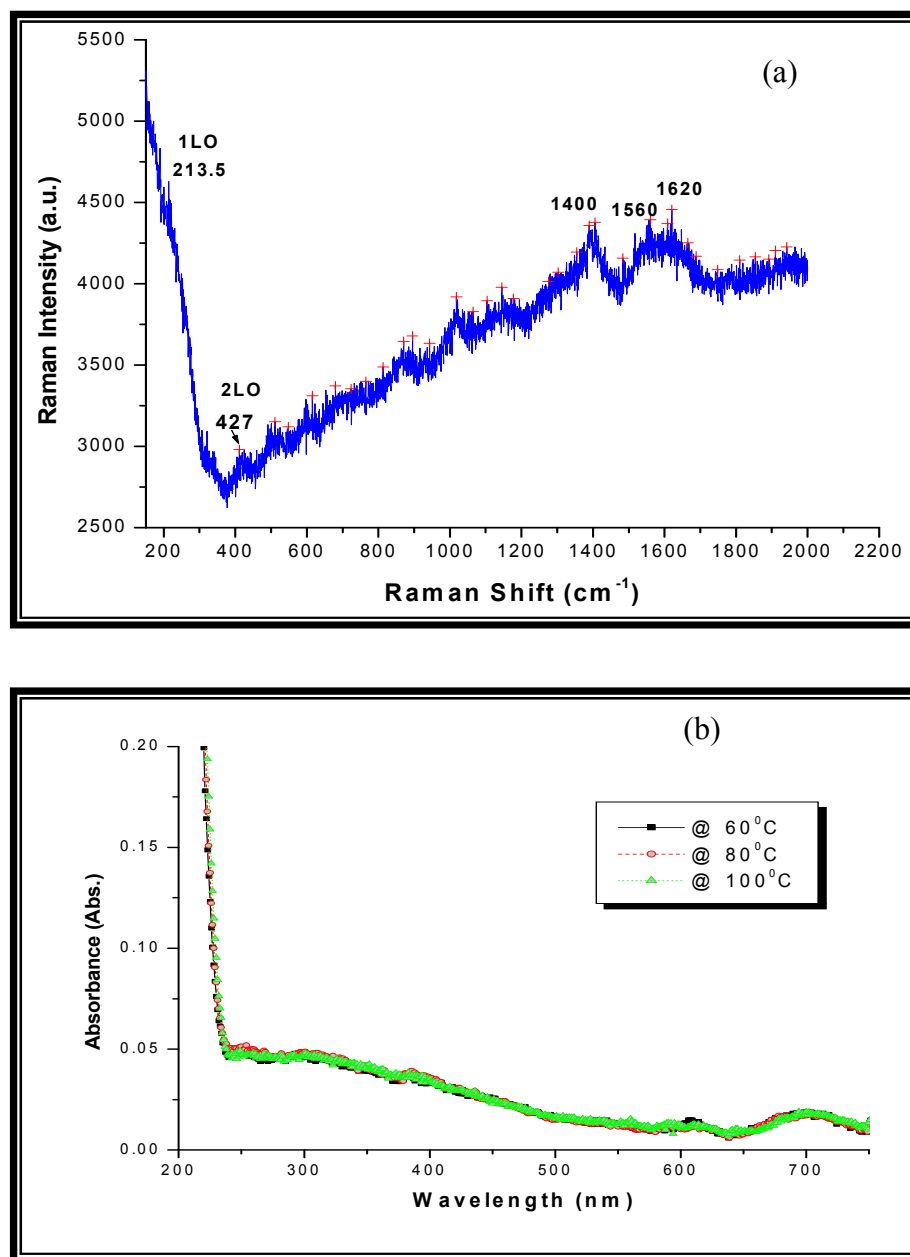


Fig. 5. (a) Raman Spectra of Ag_2S Fork architectures and (b) UV-vis Spectra of samples at various temperatures.

The fundamental and overtone modes correspond to these vibrations match well with vibrations of low temperature α -Ag₂S phase [35]. The observation of multiple resonant Raman peaks indicates that the yielded Ag₂S nanoparticles possess good optical quality [39] and good crystallinity [40]. Peaks at 1560 cm⁻¹ and 1620 cm⁻¹, correspond to Amide II and Amide I region and Peak at 1400 cm⁻¹ corresponds to CH₂ backbone of Chitosan chain. These results confirm the incorporation of Ag₂S nanoparticles inside Chitosan matrix [41]. UV-Vis absorption spectra in the 200–600 nm region of as synthesized products at various temperatures are given in Fig. 5(b).

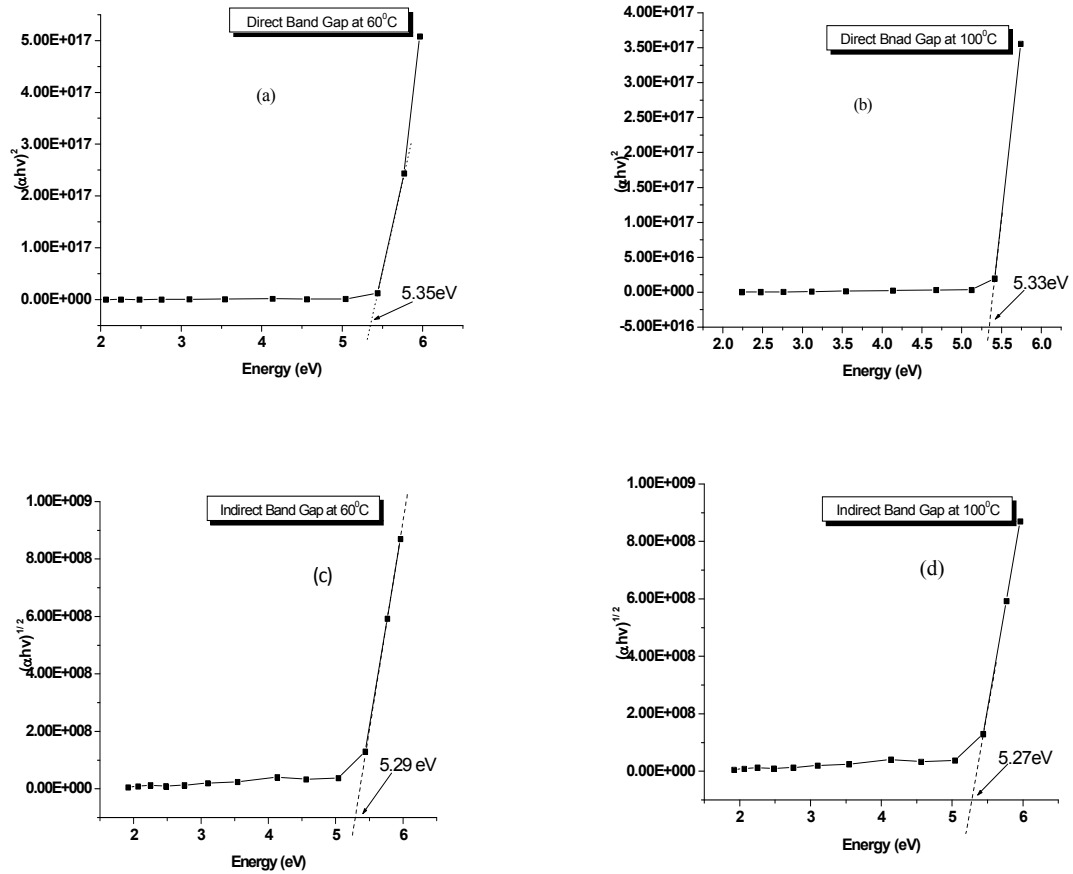


Fig. 6. Dependences $(\alpha E_{hv})^2 - E_{hv}$ and $(\alpha E_{hv})^{1/2} - E_{hv}$ for Ag₂S nanoparticles synthesized (a) Direct Band Gap at 60 °C; (b) Direct Band gap at 100 °C; (c) Indirect Band Gap at 60 °C; and (d) Indirect band Gap at 100 °C.

It is clear from the spectrum (Fig.5(b)) that there is no effect of temperature on optical absorption, since all the samples possess similar absorption spectra. All samples have broad absorption starting from 600 nm to 250 nm with monotonous increase in absorption toward the lower end of wavelength. The band gap of the synthesized Ag₂S nanoparticles were determined using theory of optical transition [42] and the band gap has been estimated by $(\alpha E_{\text{hv}})^2 - E_{\text{hv}}$ plot for direct inter band optical transition whereas $(\alpha E_{\text{hv}})^{1/2} - E_{\text{hv}}$ plot for indirect transitions. Absorption coefficients (in cm⁻¹) were calculated using the following equation:

$$\alpha = 2.303 \times 10^3 D \rho (lc)^{-1} \quad (1)$$

where D is the optical density of a solution, ρ the density of bulk Ag₂S (7.2 g cm⁻³), l the optical thickness of a cuvette (cm), c the concentration of a colloidal solution (g l⁻¹).

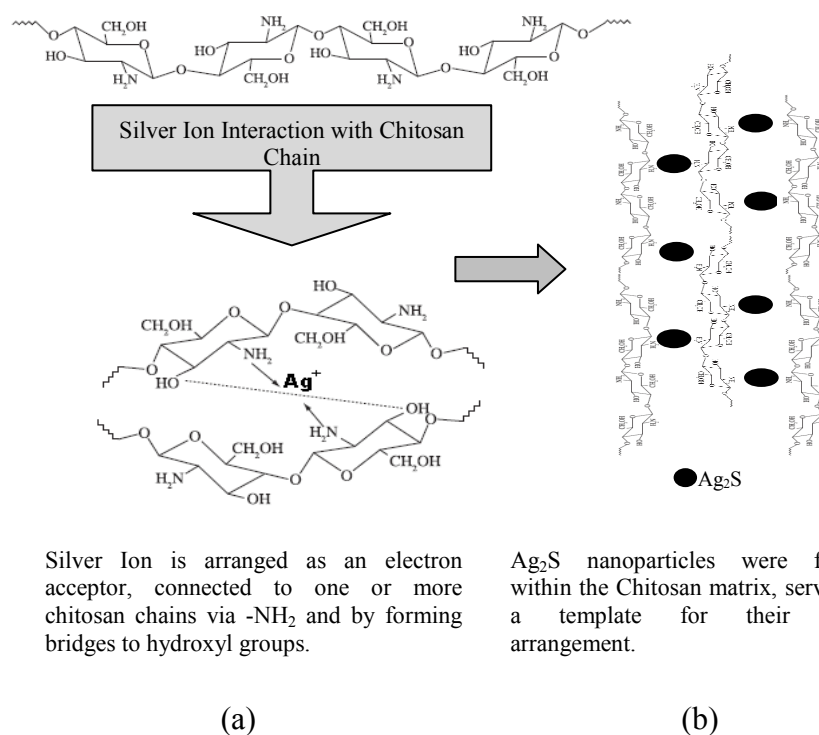
Dependence of absorption coefficient on photon energy, calculated for colloidal Ag₂S solutions at different temperatures are shown in Fig. 6. It can be seen that at both 60 °C and 100 °C temperature both direct and indirect electronic transitions can occur at the photo excitation of silver sulfide nanoparticles. As can be concluded that band gap found (5.3 eV) exceed the values of bulk silver sulfide (for bulk Ag₂S, $E_g = 0.9$ eV) [43]. Hence synthesized nanoparticles show quantum confinement effect and possesses both direct and indirect transitions. The occurrence of both direct and indirect transitions was also previously reported by Kryukov *et al* [44]. It is also clear from these results that a small red shift of 0.02 eV occurred while increasing temperature to 100 °C. The difference in direct band gap and indirect band gap in both cases were found to be constant i.e.

$$E_{\text{gd}} - E_{\text{gi}} = 0.06 \text{ eV} \quad (2)$$

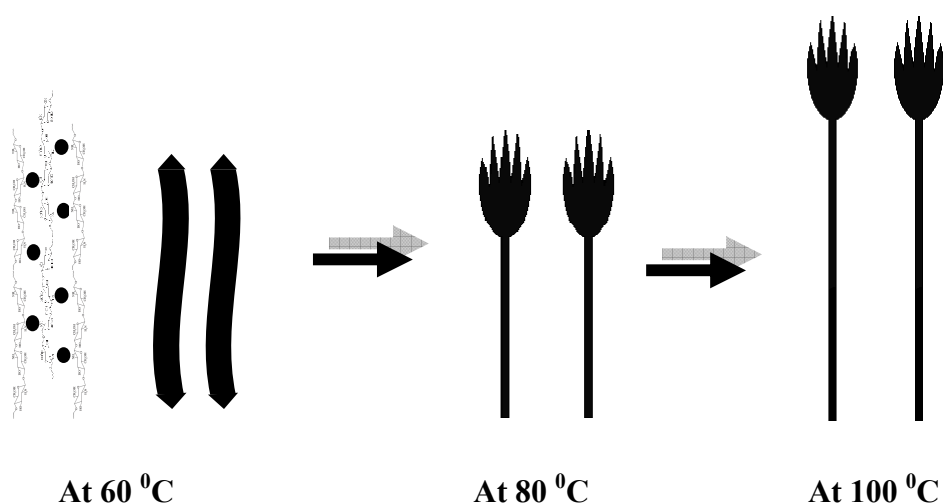
Which follows from this that transitions of both types are excited in the same particles having an average size. Hence quantum confinement effect in Ag₂S nanoparticles apparently do not affect reciprocal disposition of energy levels participating in these transitions [45].

The Proposed Growth Model and Formation Mechanism for Ag₂S Fork Architectures. To investigate the growth process of the Ag₂S Fork architectures, SEM images of the products, obtained at different ageing temperatures were analyzed. Fig. 2 shows the SEM images of the product obtained at 60 °C and at the aging temperature of 80 °C and 100 °C. It can be found that the morphology of as-synthesized samples varies from tapes and fork architectures to fork architectures with longer tails. It has been reported that chitosan interacts with inorganic ions owing to its hydrophilic and reactive nature in aqueous electrolyte solutions [30]. Chitosan and its derivatives are known for their chelating properties towards transition metal ions. Moreover, in the literature [46] it was strongly emphasized that chelation of metal ions by amine and amide groups is effective only in high basic solutions where deprotonation of –NH₂ groups takes place, which then bind the metal ions. Similar situation occurred in this case as well, where pH 10 was maintained to get stable Ag-chitosan complex. Chelation of Ag⁺ ions by –NH₂ groups is also found to be highly effective as confirmed from FTIR and Raman Spectroscopic analysis. Therefore it may be concluded that carbonyls of Chitosan units are bonded to the silver ions before reacting with Thiourea, hence preventing the Ag₂S particles from growing further after nucleation, resulting in their small size (Scheme- I). The formation of Ag₂S fork architectures could be the result of self assembly process. Schematic representation of nucleation, growth and self assembled aggregation of the Ag₂S Fork architectures are displayed in Scheme- I & II. The nucleation begins with the electrostatic attraction between the Ag⁺ ions and the negative charges of carboxylic groups (-NH₂ group) of one or more Chitosan chains and by forming bridges to hydroxyl groups [47], as illustrated in. (Scheme- I(a)). After nucleation, Ag₂S growth takes place in the free space among chitosan macromolecule chains with obvious consequences on the morphology of the inorganic deposits, owing to the effect of the

Van der Waals forces, electrostatic forces and hydrogen bonding among its chain [48,49] and resulted in non uniform tape like structures at 60 °C (Scheme- I(b)). Now as temperature further increases to 80 °C & 100 °C, spontaneous self-organization results in the formation of uniform tapes with heads having multiple arms and long tails, as depicted in Scheme-II. Increase in length of Fork structure with aging temperature shows that there is a linear assembly of Ag₂S nanoparticles using Chitosan as matrix, as the temperature increases, so does the length also increases.



Scheme-I. (a) Silver Ion – Chitosan binding Mechanism before addition of Thiourea, (b) Formation of Ag₂S linear assembly after addition of Thiourea.



Scheme-II. Growth of Fork architectures with temperature.

Since, it is evident from the SEM images that the long tape structures are formed initially at 60 °C, hence there is a probability of non uniform linear arrangement and non- symmetry along radial direction, which could result in head formation with multiple arms in the late growth stage of tapes as was seen in case of 1D growth of nanorods [50]. However in this study all this happens at the micro scale, this paves the way to work more on these findings.

Conclusion

Novel Ag₂S fork architectures were formed in-situ through reaction of silver nitrate and thiourea under the action of Chitosan in an aqueous environment. Microscopic Analysis revealed that these architectures are self-assembly of spherical Ag₂S nanoparticles of average diameter of 8nm. The XRD Pattern and SAED study revealed that as- synthesized Product is crystalline α - Ag₂S with no detected impurities. Ageing Temperature affect the final morphology of self-assembly. Spectroscopic Analysis revealed that Ag⁺ ions are coupled with the C=O bond through electrostatic interaction, this suggests that amide and carboxylic groups in chitosan chain serves as nucleation site for Ag₂S nanoparticles formation. Owing to the effect of the Van der Waals forces, electrostatic

forces and hydrogen bonds among the Chitosan macromolecules chains, the Ag₂S nanoparticles as primary units self-organize into linear tape structure which at the later stage of development under the effect of temperature creates multiple armed structures at one end hence producing fork architectures from assembly of Ag₂S nanoparticles. Raman study also confirms the formation of monoclinic α -Ag₂S acanthite phase which is thermodynamically stable below 451 K. The observation of multiple resonant Raman peaks indicated that the yielded Ag₂S nanoparticles possess good optical quality and good crystallinity. UV-visible spectral analysis revealed the existence of both direct and indirect band gap of nearly 5.3 eV, which is significantly blue, shifted from band gap of bulk Ag₂S. It is expected that this study can offer a convenient and efficient route for the development of Ag₂S architectures.

Acknowledgement

This study was carried out at M.P. Council of Science and Technology (MPCST), Bhopal under central lab facility (CLF) scheme of Govt. of Madhya Pradesh, India. Authors acknowledge the help of Dr. Ishrat Alim of CLF of MPCST during Synthesis and Characterization through FTIR and UV.

References

- [1] Kumar R.; Prakash K. H.; Cheang ;Gower P. L. and . Khor K. A, Chitosan-mediated crystallization and assembly of hydroxyapatite nanoparticles into hybrid nanostructured films. J. R. Soc. Interface 5 (2006) 427-439.
- [2] R. Singh, V. M. Maru, P. S .J. Moharir, Complex chaotic systems and emergent phenomena. J. Nonlinear Sci. 8 (1998) 235-259.
- [3] Adachi, Three-Dimensional Self-Assembly of Gold Nanocolloids in Spheroids Due to Dialysis in the Presence of Sodium Mercaptoacetate. E. Langmuir 16 (2000) 6460.

-
- [4] Y Chen, Z Rosenzweig, Luminescent CdSe quantum dot doped stabilized micelles. *Nano Lett.* 2 (2002) 1299-1302.
- [5] Y. Chen, T. Ji, Z. Rosenzweig, Synthesis of Glyconanospheres Containing Luminescent CdSe–ZnS Quantum Dots. *Nano Lett.* 3 (2003) 581-584.
- [6] T.Yonezawa, H. Matsune, N. Kimizuka, Formation of Isolated Spherical Three Units by Using an Inorganic Wrapping Technique. *Adv. Mater.* 15 (2003) 499.
- [7] C. F. J. Faul, M. Antonietti, Ionic Self-Assembly: Facile Synthesis of Supramolecular Materials. *Adv. Mater.* 15 (2003) 673-683.
- [8] M. G. Ryadnov, B.Ceyhan, C. M. Niemeyer, D. N. Woolfson, “Belt and Braces”: A Peptide-Based Linker System of de Novo Design. *J. Am.Chem. Soc.* 125 (2003) 9388-9394.
- [9] M. Maye Mathew, Jin Luo, I-Im S. Lim., Li Han, Nancy N. Kariuki, Rabinovich Daniel, Tianbo Liu, and Chuan-Jian Zhong. Size-Controlled Assembly of Gold Nanoparticles Induced by a Tridentate Thioether Ligand . *J. Am. Chem. Soc.* 125 (2003) 9906-9907.
- [10] M. Maye Mathew, I-Im S. Lim,Jin Luo, Zia Rab, Daniel Rabinovich, Tianbo Liu and Chuan-Jian Zhong. Mediator–Template Assembly of Nanoparticles. *J. Am. Chem. Soc.* 127 (2005)1519-1529.
- [11] M. M. Stevens, N. T.Flynn, C.Wang, T. D.A., Langer, R Coiled-Coil-Based Assembly of Gold Nanoparticles. *Adv. Mater.* 16 (2004) 915-918.
- [12] T. Mokari, H. Sertchook, A. Aharoni, Y. Ebenstein, D. Avnir, U. Banin, Nano@micro: General Method for Entrapment of Nanocrystals in Sol–Gel-Derived Composite Hydrophobic Silica Spheres. *Chem. Mater.* 17 (2005) 258-263.
- [13] I. Hussain, Z. Wang, A. I. Cooper, M. Brust, Formation of Spherical Nanostructures by the Controlled Aggregation of Gold Colloids. *Langmuir* 22 (2006) 2938-2941.
- [14] J. N. Cha, H. Birkedal, L. E. Euliss, M. H. Bartl, M. S. Wong, T. J.Deming, G. D. Stucky, Spontaneous Formation of Nanoparticle Vesicles from Homopolymer Polyelectrolytes. *J. Am. Chem. Soc.* 125 (2003) 8285.

-
- [15] R. Shenhar, T. B. Norsten, V. M. Rotello, Polymer-Mediated Nanoparticle Assembly: Structural Control and Applications. *Adv. Mater.* 17 (2005) 657-669.
- [16] C. Wang, X. Zhang, X. Qian, W. Wang, Y. Qian, Ultrafine powder of silver sulfide semiconductor prepared in alcohol solution. *Mater. Res. Bull.* 33 (1998) 1083-1086.
- [17] G. Hodes, J. Manassen, D. Cahen, Photoelectrochemical energy conversion and storage using polycrystalline chalcogenide electrodes *Nature* 261 (1976) 403-404.
- [18] S. Kitova, J. Eneva, A. Panov, H. Aefke, Infrared Photography Based on Vapour-Deposited Silver Sulfide Thin Films *J. Imag. Sci. Technol.* 38 (1994) 484-488.
- [19] S. Hull, D. A. Keen, D. S. Sivia, P. A. Madden, M. Wilson, The high-temperature superionic behaviour of Ag_2S . *J. Phys. Condens. Matter.* 14 (2002) 9-17.
- [20] L. Motte, F. Billoudet, E. Lacaze, J. Douin, M. P. Pileni Self-Organization into 2D and 3D Superlattices of Nanosized Particles Differing by Their Size *J. Phys. Chem. B.* 101 (1997) 138-44.
- [21] L. Motte and M. P. Pileni Self assemblies of silver sulfide nanocrystals: influence of length of thio-alkyl chains used as coating agent. *Appl. Surf. Sc.* 164 (2000) 60-7.
- [22] F. Gao, Q. Lu, S. Komarneni, Interface Reaction for the Self-Assembly of Silver Nanocrystals under Microwave-Assisted Solvothermal Conditions. *Chem. Mater.* 17 (2005) 856-860.
- [23] F. Gao, Q. L. D. Zhao, Controllable assembly of ordered semiconductor Ag_2S nanostructures. *Nano Lett.* 3 (2003) 85-88.
- [24] C. Rui, N. T. Nuhfer, Laura Moussa, H. R. Morris, P. M. Whitmore, Silver sulfide nanoparticle assembly obtained by reacting an assembled silver nanoparticle template with hydrogen sulfide gas., *Nanotechnology.* 19 (2008) 455604.
- [25] J. F. Zhu, Y. J. Zhu, M. G. Ma, L. X. Yang, L. Ga, Simultaneous and Rapid Microwave Synthesis of Polyacrylamide–Metal Sulfide (Ag_2S , Cu_2S , HgS) Nanocomposites. *J. Phys. Chem. C.* 111 (2007) 3920-3926.

-
- [26] D.K. Bozanić , V. Djoković , J. Blanus , P.S. Nair , M.K. Georges , T. Radhakrishnan , Preparation and properties of nano-sized Ag and Ag₂S particles in biopolymer matrix. *Eur Phys J E Soft Matter*. 22 (2007) 51-9.
- [27] M. Green, N. Allsop, G.Wakefield, P. Dobson, J.L. Hutchison, Trialkylphosphine oxide/amine stabilised silver nanocrystals - the importance of steric factors and Lewis basicity in capping agents *J. Mater. Chem*. 12 (2002) 2671-2674.
- [28] J. Xiao, Y. Xie , R. Tang, W. Luo, Template-based synthesis of nanoscale Ag₂E (E ~ S, Se) dendrites, *J. Mater. Chem*. 12(2002) 1148-1151.
- [29] Y. Hyunmin, Li-Qun Wu, E. B. William, G. Reza, W. R. Gary, N. C. James, F. P. Gregory, Biofabrication with chitosan. *Biomacromolecules*. 6 (2005) 2881-2894.
- [30] A. J Varma, S. V. Deshpande, J. F. Kennedy, Metal complexation by chitosan and its derivatives: a review. *Carbohydrate Polym*. 55 (2004)77-93.
- [31] G. A. Wiegers, *Am. Mineral*. 56 (1971)1882-1888.
- [32] Y. Ma, T. Zhou, C. Zhao, Preparation of Chitosan-nylon- 6 blended membranes containing silver ions as antibacterial materials, *Carbohydr Res*. 343 (2008) 230-237.
- [33] Y. F. Zhu, D. H. Fan, and W. Z. Shen, Chemical Conversion Synthesis and Optical Properties of Metal Sulfide Hollow Microspheres, *Langmuir*, 24 (2008)11131-11136.
- [34] C. J. Sandroff, S. Garoff, and K. P. Leung, Surface-enhanced Raman study of the solid/liquid interface: Conformational changes in adsorbed molecules *Chem. Phys. Lett*. 96 (1983) 547-551.
- [35] M. Osada, K. Terabe, C. Liang and T. Hasegawa, Nanoscale characterization of defect structures on Ag₂S/Ag nanowires, 214th ECS Meeting, B10 - Solid State Ionic Devices 6 - Nano Ionics, 2008.
- [36] A. Goswami, *Thin Film Fundamentals*, New Age International, New Delhi, 1996.

-
- [37] D. Routkevitch, T. Bigioni, M. Moskovits, J.M. Xu, Electrochemical Fabrication of CdS Nanowire Arrays in Porous Anodic Aluminum Oxide Templates. *J. Phys. Chem.* 100 (1996) 14037-14047.
- [38] J. Lee, *Thin solid Films*, 170 (2000) 451.
- [39] B. Kumar, H. Gong, S.Y. Chow, S. Tripathy, Y. N. Hua, Photoluminescence and multiphonon resonant Raman scattering in low-temperature grown ZnO nanostructures. *Appl. Phys. Lett.* 89 (2006) 071922.
- [40] A.G. Milekhin, L.L. Sveshnikova, T.A. Duda, Quantum dots of metal sulfides and zinc oxide in organic matrices Optical Phonons in Nanoclusters Formed by the Langmuir-Blodgett Technique. *Chinese J. of Phy.* 49 (2011) 63.
- [41] Jacob D. Goodrich; William T. Winter, *r-Chitin Nanocrystals Prepared from Shrimp Shells and Their Specific Surface Area Measurement*, *Bio-macromolecules*. 8 (2007) 252-257.
- [42] K. Seeger, *Semiconductor Physics*, Springer-Verlag, Berlin, Heidelberg, New York, London, 1991.
- [43] N.B. Hannay (Ed.), *Semiconductors*, Reinhold Publishing, 1962.
- [44] A.I. Kryukov; N.N. Zin'chuk; A.V. Korzhak; S.Ya. Kuchmii Quantum Size Effects and Nature of Photoprocesses in Nanoparticles of Ag₂S *Theor. Experim. Chem.* 37 (2001) 296-303.
- [45] Y. Wang, N. Herron, Nanometer-sized semiconductor clusters: materials synthesis, quantum size effects, and photophysical properties. *J. Phys. Chem.* 95 (1991) 525-532.
- [46] H. Sigel, R. B. Martin, Coordinating properties of the amide bond. Stability and structure of metal ion complexes of peptides and related ligands. *Chem. Rev.* 82 (1982) 385-426.
- [47] X. Wang, Y. Du, L. Fan, H. Liu, and Y. Hu, Nanometer-sized semiconductor clusters: materials synthesis, quantum size effects, and photophysical properties. *Polymer Bulletin* 55 (2005) 105-113.

-
- [48] B. Olenyuk, J. A. Whiteford, A. Fechtenkotter, P. Stang, Self-assembly of nanoscale cuboctahedra by coordination chemistry, *Nature*. 398 (1999) 796-799.
- [49] J. M. Lehn, *Supramolecular chemistry and chemical synthesis. From molecular interactions to self-assembly* NATO ASI Ser. Ser. E. 320 (1996) 511.
- [50] L. Manna, E. C. Scher, A. P. Alivisatos, Synthesis of Soluble and Processable Rod-, Arrow-, Teardrop-, and Tetrapod-Shaped CdSe Nanocrystals, *J. Am. Chem. Soc.* 122 (2000) 12700.